Iranian Journal of Medical Physics

ijmp.mums.ac.ir

Impact of Three Dimensional-Conformal Radiation Therapy (3D-CRT) Fractionation Technique on Radiobiological Effects and Risk of Secondary Cancers: A Case Study of Post-Mastectomy Breast Cancer

Endarko Endarko[1*], Dafa Miftahuddin[1], Aditya Prayugo Hariyanto[1], Aloysius Mario Yudi Putranto[2], Dewa Ngurah Yudhi Prasada[2], Ida Ayu Putu Inten Gayatri[2]

1. Laboratory of Medical Physics and Biophysics, Department of Physics, Institut Teknologi Sepuluh Nopember, Kampus ITS – Sukolilo Surabaya, 60111, East Java, Indonesia.
2. Department of Radiation Oncology, MRCCC Siloam Hospitals, Jakarta, Indonesia

ARTICLE INFO

Article type:
Original Paper

Article history:
Received: Mar 05, 2023
Accepted: Aug 23, 2023

Keywords:
Radiation Dose
Fractionation Radiotherapy
Radiation-Induced Cancer
Radiobiology

ABSTRACT

Introduction: The study aimed to analyze and determine impact of the 3D-CRT fractionation on risk of secondary cancer.

Material and Methods: This study used a patient-specific anthropomorphic phantom, and radiation was performed using the Three Dimensional-Conformal Radiation Therapy Field in Field (3D-CRT FinF) technique with conventional, hypofractionation, and hyperfractionation with a dose of 200 cGy, 260 cGy, and 160 cGy in 25, 16, and 30 fractions respectively. It focused on the contralateral breast, contralateral lung, and ipsilateral lung as Organs at Risk (OAR). In addition, the Dose Volume Histogram (DVH) value, normal tissue complication probability (NTCP), and risk of secondary cancer were evaluated.

Results: The results showed that the average dose value (D_{mean}) for ipsilateral lung with hypofractionation was smaller than conventional and hyperfractionation of 1519.8, 1826.7, and 1753.6 cGy, respectively. Furthermore, hypofractionation also reduced radiobiological effects by 50% in the ipsilateral lung with an NTCP value of 0.01% compared to conventional and hyperfractionation with a value of 0.02%. Hypofractionation reduces the risk of secondary cancer in the contralateral breast, contralateral lung, and ipsilateral lung by 16.38, 17, and 22.31% compared to conventional fractionation and 12.75, 13.54, and 21.34% compared to hyperfractionation, respectively.

Conclusion: The dose profiles in OAR was smaller in treatment planning with hypofractionation. EBT3 film verification results showed that the ipsilateral lung received more doses than planned, with an insignificant difference ($p>0.05$). In radiobiology, the ipsilateral lung has the highest probability of complications in treatment planning with conventional fractionation and hyperfractionation.

►*Please cite this article as:*
Endarko E, Miftahuddin D, Hariyanto AP, Putranto AMY, Prasada DNY, Gayatri IAPI. Impact of Three Dimensional-Conformal Radiation Therapy (3D-CRT) Fractionation Technique on Radiobiological Effects and Risk of Secondary Cancers: A Case Study of Post-Mastectomy Breast Cancer. Iran J Med Phys 2024; 21: 160-167. 10.22038/IJMP.2023.71076.2252.

Introduction

Breast cancer is very common in women and can be treated with Breast-conserving Therapy (BCT), namely mastectomy followed by radiotherapy [1].

Radiotherapy is a treatment that utilizes ionizing radiation to damage DNA in cancer and causes cell death [2]. In this treatment, irradiation is delivered in stages to give healthy cells time to recover after exposure. Three types of fractionation used in radiotherapy are conventional fractionation with a dose of 200 cGy per fraction, hyperfractionation with a dose of less than 200 cGy per fraction, and hypofractionation with a dose of more than 200 cGy per fraction [3, 4].

The main principle in radiotherapy is to provide the maximum and minimum possible dose to the target cells and the surrounding tissue. Most treatment planning systems (TPSs) have some limitations in predicting surface doses in the skin, heterogeneous material interfaces, cavities, and low-density regions such as the lung. Radiation therapy for breast cancer involves complex anatomy and various tissues with varying densities, including lung, soft tissue, bone, and air [5, 6]. In practice, the tissue around the target cell still receives an unplanned dose of radiation from the light path penetrating the target cell or due to radiation scattering. Therefore, it can cause secondary cancer after radiotherapy treatment [7]. In addition to considering the value of the dose distribution on the DVH, treatment planning also needs to consider the radiobiological effects and the risk of secondary cancer. This is crucial because it will affect long-term patient survival [8].

*Corresponding Author: Tel: +62-31-5943351; Fax: +62-31-5943351; Email: endarko@physics.its.ac.id

Many studies regarding the risk of secondary cancer have been carried out to compare radiotherapy techniques. The studies were conducted by Lee et al. [9], Han et al. [10], Haciislamoglu et al. [8], and Zhang et al. [1], who compared the techniques of 3D-CRT FinF, intensity-modulated radiotherapy (IMRT), and volumetric-modulated arc therapy (VMAT). In conventional fractionation (200 cGy), 3D-CRT radiotherapy has a lower risk of secondary cancer than other techniques. This is because the IMRT and VMAT techniques use more radiation fields, and the incidence of scattering doses in normal tissue is higher than in the 3D-CRT technique [11]. Meanwhile, 3D-CRT is a tangential technique commonly used with fields formed irregularly according to the tumor's shape from CT-scan images in treatment planning [12]. It aims to provide a high suitability and homogeneity evaluation at the target dose.

Even though it has a small risk, the 3D-CRT technique with conventional fractions has a risk of secondary cancer and radiobiological effects on organs at risk [8]. Sitathanee et al., in a study on prostate cancer radiotherapy, stated that modification of conventional fractionation to hypofractionation could reduce the risk of secondary cancer in primary radiation [11]. Meanwhile, Layton stated that hyperfractionation could lessen the potential for toxicity to the surrounding tissue due to the use of small doses [13]. Previous studies rarely compared variations in fractionation types in breast cancer radiotherapy using the 3D-CRT technique against the risk of secondary cancer.

Therefore, this study aims to analyze and determine the impact of using the 3D-CRT FinF fractionation radiotherapy technique for post-mastectomy left breast cancer cases. The DVH value, NTCP, Organ Equivalent Dose (OED), and Excess Absolute Risk (EAR) are also investigated to evaluate the impact of radiotherapy fractionation parameters.

Materials and Methods

This study began with a patient-specific chest phantom made from Polylactic Acid (PLA) referred to the registered patent No. P00202214775 (Figure1a) [14]. Images scanned with the Philips Brilliance Big Bore CT-Simulator were imported into the Eclipse v.11 TPS software for further segmentation on the target and OAR sections, as seen in Figure 1b. Furthermore, three radiotherapy treatment plans were made using the 3D-CRT FinF technique with a nominal voltage of 6 and 10 MV through the LINAC Clinac iX 2300 series 6198 with the conventional fraction (25×200 cGy), hypofractionation (16×260 cGy) and hyperfractionation (30×160 cGy). The four beam fields used were lateral and medial for the Chest-Wall section with an energy of 6 MV and the anterior and posterior fields with an energy of 6 MV and 10 MV for the node section, as shown in Figure 2.

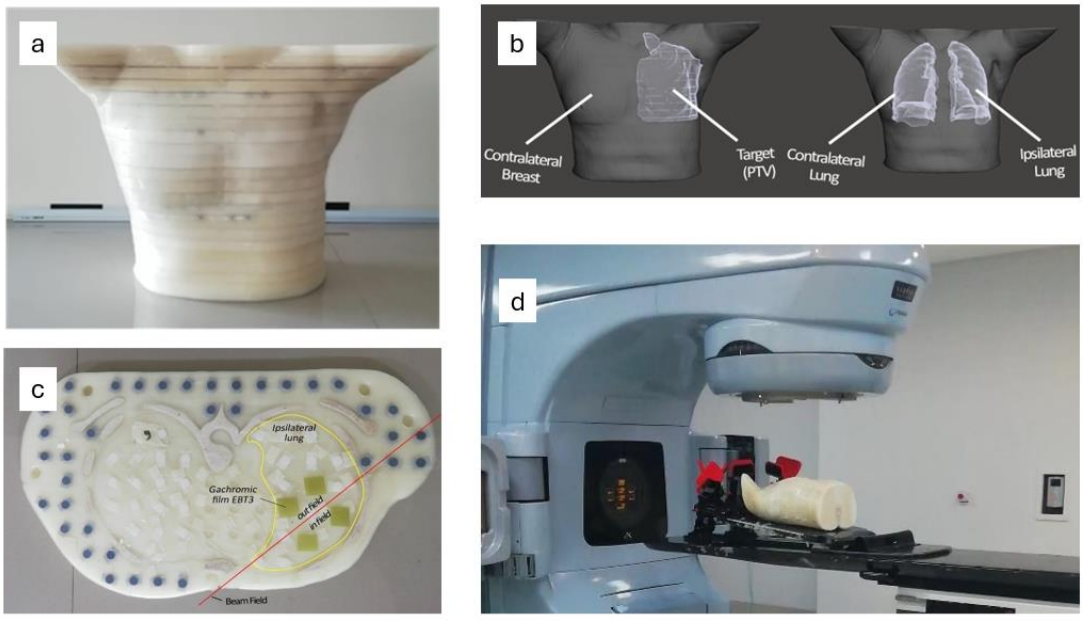

Figure 1. (a) Fabricated patient-specific chest phantom and (b) the target section and the OAR comprise the study's contralateral breast, contralateral lung, and ipsilateral lung, and (c) slice number 9 is counted from the top of the phantom, (d) patient-specific chest phantom irradiated with a linac.

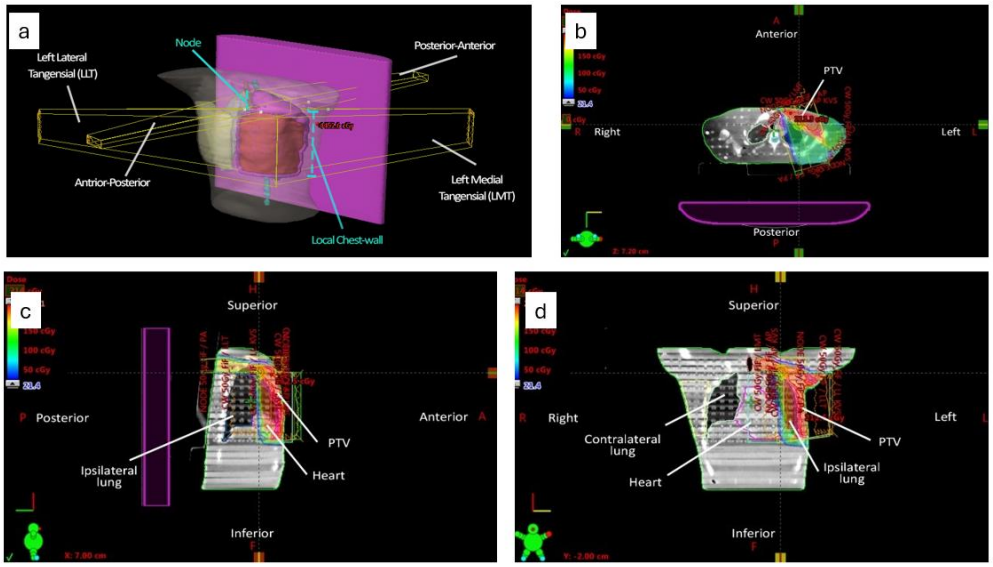

Figure 2. Simulation results of radiation treatment planning with 3D-CRT FinF technique: a) the field of local chest-wall and node sections, b) axial plane, c) sagittal plane, and d) coronal plane

DVH for the segmented sections was obtained for the three treatment plans, which were then analyzed for the distribution of doses for each OAR. Meanwhile, the analysis was based on the mean dose values for each OAR and pneumonia risk in the contralateral and ipsilateral lung. In this study, one fraction of the dose was measured in the ipsilateral lung using radiochromic films (GAFCHROMIC™ EBT3; Ashland Specialty Ingredients, Bridgewater, NJ, USA) to ascertain the similarity of the planned and actual doses received by the patient. Measurements were made by placing 2 × 2 cm2 EBT 3 films on the infield and outfield sections of the ipsilateral lung, as shown in Figure 1c. The dose values of the film measurements on the infield and outfield of the ipsilateral lung were then compared with the profile values on the treatment plan, and the error was calculated. The statistical test was used to determine a significant difference in the value of the dose. Using IBM SPSS Statistics 25, statistical tests were carried out using the independent sample t-test method with a significance level of 5%.

Radiobiological effect analysis was performed by calculating the NTCP model of Gay and Niemierko using the RADBIOMOD software. In the Gay–Niemierko model, the calculation is based on the Equivalent Uniform Dose (EUD), which assumes different dose distributions at a target volume can be equivalent when the same radiobiological effects are produced [15]. In secondary cancer risk, the values of the OED and EAR of Mechanistic Schneider models are used to evaluate a therapeutic plan. This is based on the radiation-induced dose-response model of cancer risk in Risk Equivalent Dose (RED). Meanwhile, RED combines radiobiological parameters in the form of cell killing (α') with repopulation constant (R) to calculate the effect of dose fractionation and secondary cancer induction rates derived from data on Hodgkin's patients and survivors of the Japanese atomic bombing [16].

The value of the dose tolerance parameter for 50% compilation when the entire tissue is irradiated homogeneously (TD_{50}) and the tissue-specific parameter (γ_{50}) used is 24.5 and 2 for the contralateral and ipsilateral lungs [15]. The secondary cancer risk analysis was carried out by calculating the OED and EAR values for each OAR with the Mechanistic Schneider model for the three treatment plans. The α, R, and β_{EAR} values for the contralateral breast were 0.44 Gy^{-1}, 0.15, and 9.2, respectively. In contrast, the α, R, and β_{EAR} values for the contralateral and ipsilateral lungs were 0.42 Gy^{-1}, 0.83, and 7.5, with α/β values based on the results of fitting data on Japanese atomic bomb survivors and radiotherapy patients with Hodgkin's disease [17].

The OED value is calculated using the following equation [17]:

$$OED = \frac{1}{V_T}\sum V_{D_i} RED_{D_i} \tag{1}$$

Where V_T is the total volume of organ V_D, V_{Di} is the volume of organs exposed to the D_i dose, and RED_{Di} is the RED for the dose received by V_{Di} [17].

RED is calculated by considering α', the cell killing parameter, and the fractionation effect, which includes the cell repopulation constant (R) for carcinoma induction using the Berik equation [18].

$$RED(D) = \frac{e^{-\alpha' D}}{\alpha' R}\left(1 - 2R + R^2 e^{\alpha' D} - (1-R)2e^{-\frac{\alpha' R}{1-R}D}\right) \tag{2}$$

The value of $\alpha'$is calculated using the following equation [18]:

$$\alpha' = \alpha + \beta d = \alpha + \beta \frac{D}{D_T} d_T \tag{3}$$

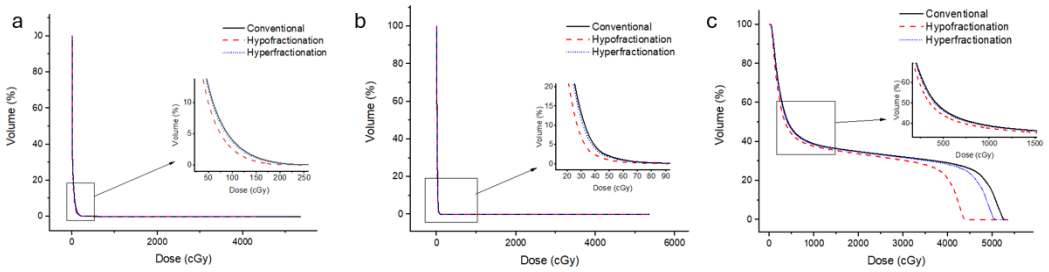

Figure 3. (a) DVH in the contralateral breast, (b) DVH in the contralateral lung, and (c) DVH in the ipsilateral lung for each type of fractionation

Where D is the dose received by the organ (Gy), D_T is the prescribed dose for the target (Gy), and d_T is the dose determined for each fraction (Gy). Parameter α is a characteristic linear value for ready organs, while β is a quadratic value in the Linear-Quadratic α/β relationship, and used an α/β of 3 [18].

Equation (4) is used to calculate the EAR value, where radiotherapy exposure is carried out when the patient is 30 years old (age a = 30), and the risk of secondary cancer is calculated at the age of 70 years (age x = 70) since the value of the age modifier factor (μ) is 1 [17].

$$EAR_{org} = \frac{1}{V_T}\sum V_{D_i} RED_{D_i} \cdot \beta \cdot \mu(age\ x, age\ a) \quad (4)$$

β is the slope of the dose-response curve for radiation-induced secondary cancer, V_D is the volume of the DVH that received the D_i dose, RED_{Di} is the RED, and μ is the age factor [17].

Results

Dose Distribution in OAR

Treatment planning for the three types of fractionation resulted in DVH graphs for each OAR, as shown in Figure 3. The conventional plans, hypofractionation, and hyperfractionation were then compared for each OAR. On the contralateral breast, the average dose value (D_{mean}) with conventional, hypofractionation, and hyperfractionation were 18.5, 15.4, and 17.7 cGy, respectively. In the contralateral lung, the D_{mean} values for the conventional, hypofractionation, and hyperfractionation were 15.6, 12.9, and 14.9 cGy. Meanwhile, in the ipsilateral lung, the D_{mean} value was 1826.7, 1519.8, and 1753.6 cGy, respectively.

Verification of Dose Distribution in Ipsilateral Lung

The ipsilateral lung is used for dose verification because it is close to the irradiation field. Therefore, the dose received on the ipsilateral lung can reflect the suitability received by other OARs. The measurement results are then compared with the dose profile, and the error value is calculated, as shown in Table 1. Table 1 shows that the ipsilateral lung dose in the in-field section absorbs more doses than the outfield for treatment planning. The 3D-CRT tangential plane has cut the high dose distribution in the ipsilateral lung.

NTCP Analysis as a Radiobiological Effect

Treatment planning was analyzed using dosimetry parameters and radiobiological effects. One of the radiobiological effect parameters is the NTCP of the tissue complication probability [19]. This study calculated NTCP values for the contralateral and ipsilateral lungs. The values for each treatment plan with the three types of fractionation were then compared and listed in Table 2. NTCP in the contralateral lung seemed to be 0% for each treatment plan with the three types of fractionation but varied in the ipsilateral lung.

Table 1. Comparison of film dose values with dose profiles in the ipsilateral lung for each fractionation variation in one fraction

Fractionation type	Part	Average point dose (cGy)		Error Value (%)
		Film Measurement	Profile dose	
Conventional	Infield	212.98 ± 5.57	202.27 ± 4.61	5.30
	Outfield	17.62 ± 4.59	15.23 ± 4.02	15.73
Hypofractionation	Infield	278.02 ± 14.85	258.69 ± 13.62	7.47
	Outfield	23.59 ± 7.29	21.04 ± 7.10	12.12
Hyperfractionation	Infield	175.32 ± 5.31	161.86 ± 3.27	8.32
	Outfield	13.65 ± 3.06	11.33 ± 2.60	20.48

Table 2. Results of Gay & Niemierko model NTCP calculations on conventional, hypofractionated, and hyperfractionated fractions

Fractionation type	NTCP (%)	
	Contralateral Lung	Ipsilateral Lung
Conventional	0.00	0.02
Hypofractionation	0.00	0.01
Hyperfractionation	0.00	0.02

Table 3. OED and EAR values of the Mechanistic Schneider model on OAR for conventional, hypofractionation, and hyperfractionation

Fractionation type	OED Mechanistic Model (Gy)			EAR {Mechanistic Model (per 10000 PY)}		
	Contralateral breast	Contralateral lung	Ipsilateral Lung	Contralateral breast	Contralateral lung	Ipsilateral lung
Conventional	0.39	0.13	43.67	3.60	1.00	327.52
Hypofractionation	0.33	0.11	33.94	3.01	0.83	254.48
Hyperfractionation	0.38	0.13	43.18	3.45	0.96	323.84

OED and EAR Analysis as Secondary Cancer Risk

The results of calculating OED values are listed in Table 3, and the OED calculations in Table 3 show that treatment planning with hypofractionation produces the smallest values of 0.33, 0.11, and 33.94 Gy in tissue-specific repopulation conditions. Therefore, hypofractionation provides an equivalent dose for each OAR which is smaller than other types of fractionation.

Table 3 also shows hypofractionation has a smaller EAR value than treatment planning with conventional or hyperfractionation for the entire OAR. In hypofractionation treatment, the EAR values of the contralateral breast, contralateral lung, and ipsilateral lung were 3.01, 0.83, and 254.4 per 10000 person-year, respectively. The complication reduced 16.38, 17, and 22.31% risk of secondary cancer 40 years after treatment in the contralateral breast, contralateral lung, and ipsilateral lung to the conventional fraction and reduced 12.75, 13.54, and 21.34% against hyperfractionation.

Discussion

Treatment planning with hypofractionation provides a smaller exposure to D_{mean} than other types of fractionation for each OAR. These results align with Moran's previous study of hypofractionation, where hypofractionation reduced dose exposure to OAR [20].

The distribution analysis in the contralateral and ipsilateral lung is based on the D_{mean} value and the risk of pneumonia after treatment. Pneumonia is based on the Quantitative Analysis of Normal Tissue Effects (QUANTEC), which states that the risk of developing symptomatic radiation pneumonitis in the lung is 4% and 50% when the percentage of lung volume structure receives a dose of 500 cGy (V_5) and 2000 cGy (V_{20}) below 42 and in the range of 31–40% [21].

Table 4 represents V_5 and V_{20} for each treatment plan which is processed from the DVH graphs in Figures 3(b) and 3(c). In the contralateral lung, the V_5 and V_{20} values were 0% for all types of fractionation; hence, the risk of pneumonia in that organ is minimal. However, the risk of pneumonia occurs by 10% due to part of the ipsilateral lung volume being in the irradiation plane. The lowest and highest risks are in treatment planning with hypofractionation and conventional fractions. This is in line with the study by Rastogi, which found pneumonia in only 2% of the group of patients irradiated using hypofractionation, compared to conventional fractionation, where 6% had pneumonia [22].

On verification of the distribution of doses on the ipsilateral lung, the average measured value of EBT3 film is greater than the average profile for all fractionation variations, with errors in the infield and outfield sections of 5–9% and 15–21%. Therefore, the ipsilateral lung received a larger dose than the planned amount. The dose profile values cause a significant error at several outfield points below the optimal range of EBT3 films, in which the optimum values are 20−1000 cGy [23].

Moreover, NTCP analysis on the contralateral lung showed a value of 0% for each treatment plan with all three types of fractionation. A value of 0% indicates a slight possibility of organ complications during radiotherapy treatment [24]. Treatment planning with hypofractionation also reduces 50% of the complications' possibility in the ipsilateral lung with an NTCP value of 0.01% compared to treatment with other types of fractionation at 0.02%. A low NTCP provides a low probability of normal tissue complications [15]. The results align with other studies regarding the potential risks and benefits of treating breast and prostate cancer. Hypofractionation can maintain dose equivalence regarding tumor and tissue damages [25].

For the analysis of OED and EAR as secondary cancer risks, this study showed that hypofractionation provides an equivalent dose for each OAR smaller than other types of fractionation. Haciislamoglu stated that the smaller the OED value received by the organ, the better the treatment plan [8]. Therefore, treatment planning with hypofractionation is better compared to other fractionation types.

Radiation treatment of post-mastectomy breast cancer with the 3D-CRT technique often carries a high risk of exposure to the ipsilateral lung [10, 26]. In the study comparing radiotherapy techniques to the risk of secondary cancer, the ipsilateral lung received more OED values than other OAR in the 3D-CRT technique at 3.54 Gy in the mechanical model [8]. The high value of OED in the ipsilateral lung was due to the irradiation target on the Local chest wall and nodes. It causes the ipsilateral lung volume to be in the tangential medial-lateral and anterior-posterior 3D-CRT Find beam plane, as shown in Figure 2. The distribution of doses to these organs in Figure 4 shows the amount of radiation dose deposited in the ipsilateral lung.

Meanwhile, the high EAR value in the ipsilateral lung is due to its location in the direction of the irradiation plane. In the study by Vogel, the significant contribution to secondary cancer induction can be presumed to arise from the in-field dose through the lung and large areas exposed to very low out-of-field doses [27].

Table 4. DVH curve volume percentage values in lung 3D-CRT technique for conventional, hypofractionated, and hyperfractionated fractions

Lung	Fractionation type	V_5 (%)	V_{20} (%)
Contralateral	Conventional	0	0
	Hypofractionation	0	0
	Hyperfractionation	0	0
Ipsilateral	Conventional	46.78	34.88
	Hypofractionation	43.98	33.73
	Hyperfractionation	46.11	34.64

Correlated with OED values in hypofractionation, EAR values in the ipsilateral lung, as the risk of secondary cancer at 40 years after treatment, can be reduced by 22.30% compared to conventional fractions and 21.42% when compared to hyperfractionation. A similar study was found by Sitatanaee, where modification of conventional fractionation can reduce the risk of secondary cancer in primary radiation [11].

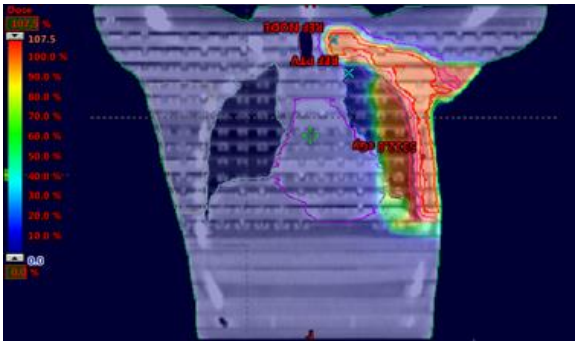

Figure 4. Dose distribution in the coronal plane using the 3D-CRT FinF technique

The measurement results were then performed by statistical tests between film measurement data and dose profiles to determine the significant difference. Meanwhile, the statistical tests were carried out using the independent samples t-test method, and the p-value of the results in the infield and outfield was at 0.10 and 0.74, respectively. The independent samples method t-test was conducted with the hypothesis (H_0), and the average difference between the two data was equal to zero with an alpha limit of 0.05. The H_0 value is rejected when the p-value is in the rejection area, or the value is smaller than the alpha value, and the data have significantly different values [28].

The results show that the p-value of the statistical test in the infield and outfield sections has a $p>0.05$. Hence, the H_0 value is acceptable with insignificant differences. Even though the film measurement results are more significant than the dose profile in treatment planning, the difference in dose values does not occur significantly in the sections. Therefore, the analysis of radiobiological effects and risk of secondary cancer can be based on the DVH value. This study has limitations on the specific case of left breast cancer patients with the 3D-CRT FinF technique with hypofractionation, which may give different risk results when analyzed in other patient cases.

Conclusion

This present study demonstrated that the dose distribution in OAR is smaller in treatment planning with hypofractionation. The results of verification of the EBT3 film showed that the ipsilateral lung received more doses than the planned one, with a non-significant difference ($p>0.05$). In radiobiology, the ipsilateral lung has the highest probability of complications in treatment planning with conventional fractionation and hyperfractionation. This is also seen in the aspect of secondary cancer, and the conventional fraction (25×200 cGy) with a prescription dose of 5000 cGy provides a higher risk in the ipsilateral lung after radiation treatment compared to hyperfractionation (30×160 cGy) and hypofractionation (16×260 cGy). The prescription dose is directly proportional to the radiobiological effects and the risk of secondary cancer.

Acknowledgment

The authors are grateful to the management of the Mochtar Riady Comprehensive Cancer Center Siloam Hospitals Semanggi, Jakarta, Indonesia, for the permission to conduct the study and collect and analyze data at the Radiotherapy Facility.

References

1. Zhang Q, Liu J, Ao N, Yu H, Peng Y, Ou L, Zhang S. Secondary cancer risk after radiation therapy for breast cancer with different radiotherapy techniques. Scientific reports. 2020 Jan 27;10(1):1220. https://doi.org/10.1038/s41598-020-58134-z.
2. Puspitasari RA, Pertiwi WI, Sholihah PM, Fariqoh WH, Kavilani N, Astuti SD. Analisis Kualitas Berkas Radiasi LINAC Untuk Effektivitas Radioterapi. Jurnal Biosains Pascasarjana. 2020;22(1):11-9. https://doi.org/10.20473/JBP.V22I1.2020.11-19.
3. Schomberg PJ, Shanahan TG, Ingle JN, Donohue JH, Kuske RR, Sternfeld WC, et al. Accelerated hyperfractionation radiation therapy after lumpectomy and axillary lymph node dissection in patients with stage I or II breast cancer: pilot study. Radiology. 1997 Feb;202(2):565-9. https://doi.org/10.1148/RADIOLOGY.202.2.9015091.
4. Marta GN, Riera R, Pacheco RL, Martimbianco AL, Meattini I, Kaidar-Person O, et al. Moderately hypofractionated post-operative radiation therapy for breast cancer: Systematic review and meta-analysis of randomized clinical trials. The Breast. 2022 Apr 1;62:84-92. https://doi.org/10.1016/J.BREAST.2022.01.018.

5. EPimenta EB, Nogueira LB, de Campos TP. Dose measurements in a thorax phantom at 3DCRT breast radiation therapy. reports of practical Oncology and radiotherapy. 2021;26(2):242-50. https://doi.org/10.5603/RPOR.a2021.0037.
6. Hedin E, Bäck A, Chakarova R. Impact of lung density on the lung dose estimation for radiotherapy of breast cancer. Physics and Imaging in Radiation Oncology. 2017 Jul 1;3:5-10. https://doi.org/10.1016/j.phro.2017.07.001.
7. Khabaz R. Phantom dosimetry and cancer risks estimation undergoing 6 MV photon beam by an Elekta SL-25 linac. Applied Radiation and Isotopes. 2020 Sep 1;163:109232. https://doi.org/10.1016/j.apradiso.2020.109232.
8. Haciislamoglu E, Cinar Y, Gurcan F, Canyilmaz E, Gungor G, Yoney A. Secondary cancer risk after whole-breast radiation therapy: field-in-field versus intensity modulated radiation therapy versus volumetric modulated arc therapy. The British journal of radiology. 2019 Oct 1;92(1102):20190317. https://doi.org/10.1259/BJR.20190317/ASSET/IMAGES/LARGE/BJR.20190317.G003.JPEG.
9. Lee B, Lee S, Sung J, Yoon M. Radiotherapy-induced secondary cancer risk for breast cancer: 3D conformal therapy versus IMRT versus VMAT. Journal of radiological protection. 2014 Apr 4;34(2):325. https://doi.org/10.1088/0952-4746/34/2/325.
10. Han EY, Paudel N, Sung J, Yoon M, Chung WK, Kim DW. Estimation of the risk of secondary malignancy arising from whole-breast irradiation: comparison of five radiotherapy modalities, including TomoHDA. Oncotarget. 2016 Apr 4;7(16):22960.
11. Sitathanee C, Tangboonduangjit P, Dhanachai M, Suntiwong S, Yongvithisatid P, Rutchantuk S, et al. Secondary cancer risk from modern external-beam radiotherapy of prostate cancer patients: Impact of fractionation and dose distribution. Journal of Radiation Research. 2021 Jul;62(4):707-17. https://doi.org/10.1093/JRR/RRAB038.
12. Apriantoro NH, Wibowo BS, Irsal M, Kasih PC. Result Analysis Of Treatment Planning System Between 3-Dimensional Conformal Radiation Therapy Technique And Intensity Modulated Radiation Therapy Technique In Nasopharyngeal Cancer Cases. Sanitas. 2017 Oct 26;8(1):29-34.
13. Layton C, Twadell S, McDonald KA, Genuit T, Richter S. Preoperative Accelerated Hyperfractionated Whole-Breast Radiation as Treatment for Secondary Angiosarcoma of the Breast After Prior Accelerated Hypofractionated Whole-Breast Radiation Therapy: A Case Report and Review of the Literature. Advances in Radiation Oncology. 2022 Jul 1;7(4):100846. https://doi.org/10.1016/j.adro.2021.100846.
14. Endarko E, Hariyanto AP. 3D Fantom Antropomorfik Untuk Jaminan Kualitas Radioterapi Pada Kasus Kanker Payudara Pasca-Mastektomi. 2021 Indonesia Patent: P00202102195.
15. Gay HA, Niemierko A. A free program for calculating EUD-based NTCP and TCP in external beam radiotherapy. Physica Medica. 2007 Dec 1;23(3-4):115-25. https://doi.org/10.1016/J.EJMP.2007.07.001.
16. Murray LJ, Thompson CM, Lilley J, Cosgrove V, Franks K, Sebag-Montefiore D, et al. Radiation-induced second primary cancer risks from modern external beam radiotherapy for early prostate cancer: impact of stereotactic ablative radiotherapy (SABR), volumetric modulated arc therapy (VMAT) and flattening filter free (FFF) radiotherapy. Physics in Medicine & Biology. 2015 Jan 15;60(3):1237. https://doi.org/10.1088/0031-9155/60/3/1237.
17. Schneider U, Sumila M, Robotka J. Site-specific dose-response relationships for cancer induction from the combined Japanese A-bomb and Hodgkin cohorts for doses relevant to radiotherapy. Theoretical Biology and Medical Modelling. 2011 Dec;8:1-21. https://doi.org/10.1186/1742-4682-8-27.
18. 18. Schneider U, Zwahlen D, Ross D, Kaser-Hotz B. Estimation of radiation-induced cancer from three-dimensional dose distributions: Concept of organ equivalent dose. International Journal of Radiation Oncology* Biology* Physics. 2005 Apr 1;61(5):1510-5. https://doi.org/10.1016/j.ijrobp.2004.12.040.
19. Taheri H, Akhavan A, Tavakoli M, Moghareabed R, Kianinia M. Dosimetric Comparison and TCP-NTCP Modeling for Lung, Heart, Left Anterior Descending, and Right Coronary Artery in Left-sided Breast Cancer Conventional and Hypofractionated Radiotherapy. International Journal of Cancer Management. 2021 Dec 31;14(12). https://doi.org/10.5812/IJCM.117987.
20. Moran MS, Truong PT. Hypofractionated radiation treatment for breast cancer: The time is now. The Breast Journal. 2020 Jan;26(1):47-54. https://doi.org/10.1111/TBJ.13724.
21. Emami B, Lyman J, Brown A, Cola L, Goitein M, Munzenrider JE, et al. Tolerance of normal tissue to therapeutic irradiation. International Journal of Radiation Oncology* Biology* Physics. 1991 May 15;21(1):109-22. https://doi.org/10.1016/0360-3016(91)90171-Y.
22. Rastogi K, Jain S, Bhatnagar AR, Bhaskar S, Gupta S, Sharma N. A comparative study of hypofractionated and conventional radiotherapy in postmastectomy breast cancer patients. Asia-Pacific Journal of Oncology Nursing. 2018 Jan 1;5(1):107-13. https://doi.org/10.4103/APJON.APJON_46_17.
23. Ashland. GAFCHROMIC ™ DOSIMETRY MEDIA, TYPE EBT-3. 2018. [Online]. Available: http://www.gafchromic.com/gafchromic-film/radiotherapy-films/EBT/index.asp
24. Abi KS, Habibian S, Salimi M, Shakeri A, Mojahed MM, Gharaati H. Tumor Control Probability (TCP) and Normal Tissue Complication Probability (NTCP) in Mono and Dual-isocentric Techniques of Breast Cancer Radiation Therapy. Archives of Breast Cancer. 2021 Jul 27:192-202. https://doi.org/10.32768/ABC.202183192-202.
25. Ray KJ, Sibson NR, Kiltie AE. Treatment of breast and prostate cancer by hypofractionated radiotherapy: potential risks and benefits. Clinical oncology. 2015 Jul 1;27(7):420-6. https://doi.org/10.1016/J.CLON.2015.02.008.
26. Donovan EM, James H, Bonora M, Yarnold JR, Evans PM. Second cancer incidence risk estimates using BEIR VII models for standard and complex external beam radiotherapy for early breast cancer.

Medical physics. 2012 Oct;39(10):5814-24. https://doi.org/10.1118/1.4748332.
27. Vogel M, Gade J, Timm B, Schürmann M, Auerbach H, Nüsken F, et al. Comparison of Breast Cancer Radiotherapy Techniques Regarding Secondary Cancer Risk and Normal Tissue Complication Probability−Modelling and Measurements Using a 3D-Printed Phantom. Frontiers in Oncology. 2022 Jul 27;12:892923.
28. Gerald B. A brief review of independent, dependent and one sample t-test. International journal of applied mathematics and theoretical physics. 2018 Aug;9(2):50-4. https://doi.org/10.11648/j.ijamtp.20180402.13.